Optik xxx (2011) xxx–xxx

Contents lists available at ScienceDirect

Optik

journal homepage: www.elsevier.de/ijleo

Structure, dielectric and optical properties of p-type (PVA/CuI) nanocomposite polymer electrolyte for photovoltaic cells

E. Sheha*, H. Khoder, T.S. Shanap, M.G. El-Shaarawy, M.K. El Mansy

Physics Department, Faculty of Science, Benha University, Benha, Egypt

ARTICLE INFO

Article history:
Received 7 February 2011
Accepted 30 June 2011
Available online xxx

Keywords:
Ionic conductivity
PVA/CuI nano-composite
Optical properties

ABSTRACT

A novel PVA/CuI nanocomposite polymer electrolyte layer synthesized via the reduction of $CuCl_2$ by NaI in an aqueous PVA solution. The as-prepared films were characterized by X-ray diffraction, scanning electron microscope, as well as impedance spectroscopy. The obtained results indicated the formation of hexagonal CuI nano particles of ≈55 nm sizes embedded in the PVA matrix. In addition, the study of dielectric parameters and conductivity of PVA/CuI nanocomposite in wide range of temperature and frequency are given and discussed. The frequency dependence of ac-conductivity suggests power law with an exponent $0.026 < s < 0.73$ which predicts hopping of charge carriers. The bulk conductivity showed activation with temperature, significant values of activation energy are deduced and discussed. An average value of the energy gap width, 2.05 eV obtained using optical absorption in UV–visible spectra for PVA/CuI nanocomposite polymer electrolyte.

1. Introduction

Organic/inorganic nanocomposites are extremely promising for applications in light-emitting diodes, photodiodes, photovoltaic cells, smart microelectronic device, and gas sensors among others [1]. The properties of nanocomposites films can be adjusted by varying the composition. Their fabrication shares the same advantages of organic device technology, such as low cost production and the possibility of device fabrication on large area and flexible substrates.

PVA is a potential material having high dielectric strength, good charge storage capacity and dopant-dependent electrical and optical properties. It has carbon chain backbone with hydroxyl groups attached to methane carbons/these OH groups can be a source of hydrogen bonding and hence assist the formation of polymer composite [2].

Cuprous iodide (CuI) has attracted a great attention, as it is a versatile candidate in band gap materials (CuI, CuSCN, and $CuAlO_2$) were identified in the preparation of optical properties of thin film [3–5]. CuI belongs to the I–VII semiconductors with zinc blende structure. Conducting and optically transparent films aroused much interest in the capability of application in electronic devices such as liquid crystal displays, photovoltaic devices, photothermal collectors and so on [6]. The most interesting nature of this compound is that an inorganic semiconductor and its coordination chemistry let it readily couple with many inorganic and organic ligands as well.

The properties of semiconductor nanoparticles depend mainly on their shape and size due to high surface-to-volume ratio [7,8]. The use of polymers is a prominent method for the synthesis of semiconductor nanoparticles. The reason is that the polymer matrices provide for processability, solubility, and control of the growth and morphology of the nanoparticles.

Various approaches have been employed to prepare nanoparticles/polymer composites. Conventionally, polymerization of monomers and formation of inorganic nanoparticles were performed separately, and then the polymer and the inorganic nanoparticles were mechanically mixed to form composites [9]. However, sometimes it is difficult to disperse nanoparticles into the polymer matrix homogeneously owing to the easy agglomeration of nanoparticles and the high viscosity of polymers. Therefore, more attention has been paid to the in situ synthesis of inorganic nanoparticles in polymer matrices.

The present work aims to use an aqueous solution of PVA as host matrix for $CuCl_2$:NaI reaction to produce p-type nano CuI/ polymer nanocomposite. The study will extend to the characterization of CuI polymer composite to optimize the optical and transport properties to be the base of heterojunction in photovoltaic applications.

2. Experimental

2.1. Sample preparation

All chemicals used in the present study were provided by QualiKems Chemical Company, India. Polymer electrolyte layers were

* Corresponding author. Tel.: +20 107414705; fax: +20 3222578.
E-mail address: e_sheha@yahoo.com (E. Sheha).

0030-4026/$ – see front matter.
doi:10.1016/j.ijleo.2011.06.066

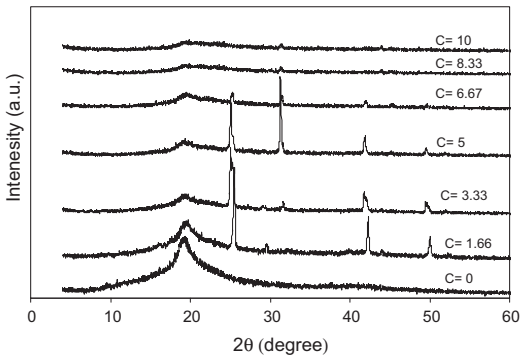

Fig. 1. XRD patterns for PVA: C (NaI/$CuCl_2$) polymer electrolytes.

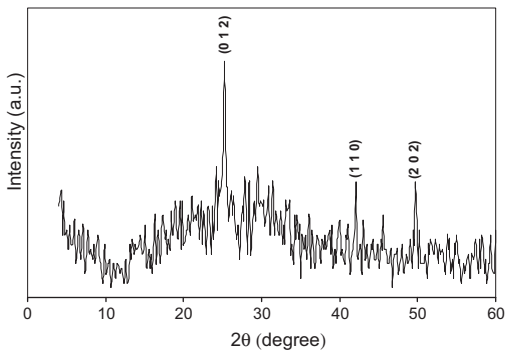

Fig. 2. XRD pattern for the solid separated CuI.

prepared by the solution cast technique. PVA solution was prepared by adding first distilled water to solid PVA $(C_2H_4O)_n$ (where $n = 1800$), and stirred by a magnetic stirrer at 70 °C for 2 h. After aging the solution for another 1 h, when the temperature dropped to room temperature, a solution of $CuCl_2$ in H_2O was first added into the PVA solution under stirring at room temperature; then different NaI solution in H_2O was added 2 h later drop wise into the reaction vessel satisfying the ratio C = NaI/$CuCl_2$, (C = 0, 1.66, 3.33, 5, 6.67, 8.33 and 10), followed by stirring for another 2 h. The production process of CuI was according to the following reaction [10]

$$2Cu^{2+} + 4I^{-} \rightarrow 2CuI + I_2$$

The as-prepared polymer electrolyte was direct cast in Petri-glass dishes and left for two weeks and then dried under evacuation at room temperature.

2.2. Characterization

In order to investigate the structure of the polymer electrolyte layers, X-ray diffraction studies were carried out using ShimADZU diffractometer type XRD 6000, wave length λ = 1.5418 Å. The CuI nanoparticles powder was separated from composite solution by centrifuge at 6000 rpm for 30 min. The precipitated powder was then washed by water several times in order to remove residual NaCl by-product and the excess of reactants, and finally the precipitant was left at room temperature to dry. The structure of precipitate was examined using X-ray diffraction. In addition, the morphology of the polymer electrolyte was examined using scanning electron microscope, SEM (JOEL-JSM Model 5600).

Thick layers of polymer electrolyte of thickness between 200 and 300 μm were subjected to conductivity measurements where silver past was used as conducting electrodes on the desired area. Electrical measurements were carried out in the temperature range 303–373 K using PM 6304 programmable automatic RCL (Philips) meter in the frequency range 0.1–100 kHz. The optical absorption of the polymer electrolyte films was measured in the wavelength range 190–1100 nm using JENWAY 6405 UV–visible spectrophotometer at room temperature.

3. Results and discussion

3.1. X-ray diffraction investigation

A typical XRD pattern of the as-prepared polymer electrolyte shown in Fig. 1, abroad peak around 19.44° observed for pure PVA. As the C ratio increases up to 5, new sharp peaks raised at 25.49°, 42.24° and 49.99° indicating the growth of CuI crystallites in the polymer matrix. Above such concentration the observed peaks disappear, besides a broadness and reduction of height of the essential peak of PVA was observed. This is in agreement with Hodge et al. [11] criterion, which established a correlation between the intensity of the peak and the degree of crystallinity.

A typical XRD pattern for the powder precipitate by centrifuge is shown in Fig. 2, it shows three diffraction peaks at 25.28°, 42.08° and 49.76° corresponding to the (0 1 2), (1 1 0) and (2 0 2) planes of CuI crystals which could be indexed to hexagonal structure (the lattice constants are, a = 4.291 Å and c = 21.48 Å), which were consistent with the literature data of JCPDS card No. 83-1145. The average particle size can be calculated using the first sphere approximation of Debye–Scherrer formula [12],

$$D = \frac{0.9\lambda}{B\cos\theta} \quad (1)$$

where D is the average diameter of the crystals, λ is the wavelength of X-ray radiation, B is the full width at half maximum intensity of the peak. The average particle size of CuI extracted by centrifuge is ~55 nm. The particle size of CuI embedded in polymer electrolyte obtained at different mentioned C ratio is shown in Table 1. These values of CuI particle sizes lie in the same range of those of precipitates 55 nm. The apparent fluctuation of the particle size of CuI phase may be attributed to the particles aggregation and/or complexation of NaI in PVA polymer matrix.

3.2. Morphology investigation

Scanning electron microscopy has been used to study the compatibility between various components of the polymer electrolytes through the detection of phase separations and interfaces. It has great influence on the physical properties of the polymer composite. Fig. 3(a and b) shows the SEM photograph of nanocomposite polymer electrolyte. The films exhibit little density of grain distribution at surface morphology. It can be seen from Fig. 3(c) that the grain aggregates with increasing C ratio. It can also be seen that some tiny pores existed between the filler–polymer interfaces. It is attributed to the compatibility between the filler and the polymer. The surface morphology of the PVA/CuI polymer electrolyte films shows many aggregates or chunks randomly distributed on

Table 1
Bulk conductivity, activation energy, particle size (P.S.) and the optical parameters (E_g and E_u) for PVA: C (NaI/$CuCl_2$) polymer electrolytes.

C (NaI/$CuCl_2$)	σ_b (S cm^{-1})	E_b (ev)	E_g (ev)	E_u (ev)	P.S. (nm)
0	3.86×10^{-9}	1.24	3.39	0.35	–
1.66	2.07×10^{-8}	0.83	1.98	0.89	36
3.33	2.56×10^{-7}	0.69	2.048	0.91	15
5	1.11×10^{-6}	0.7	1.99	1.17	57
6.67	7.65×10^{-7}	0.69	2.14	0.88	23
8.33	7.8×10^{-6}	0.5	2.047	0.91	56
10	2.48×10^{-5}	0.33	2.12	0.84	55

Please cite this article in press as: E. Sheha, et al., Structure, dielectric and optical properties of p-type (PVA/CuI) nanocomposite polymer electrolyte for photovoltaic cells, Optik - Int. J. Light Electron Opt. (2011), doi:10.1016/j.ijleo.2011.06.066

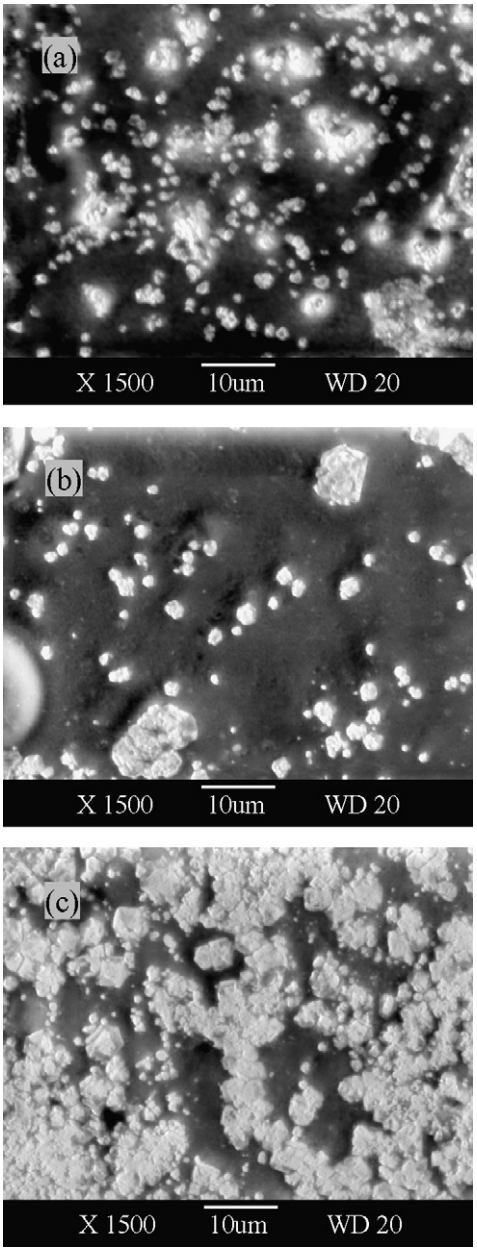

Fig. 3. SEM images of PVA: C (NaI/$CuCl_2$) polymer electrolytes: (a) $C = 3.33$, (b) $C = 6.67$ and (c) $C = 8.33$.

the top surface. It was found that the dimension of those aggregates embedded in the PVA matrix was around 1–2 μm. The results indicate that the nano-sized CuI particles tended to form aggregates and dispersed into the PVA polymer matrix.

3.3. AC spectroscopy

Fig. 4 illustrates the impedance plot of the imaginary part, Z'', against the real part, Z', for polymer electrolytes at room temperature. The impedance plot, in general, shows an arc (semicircle), its centre below the Z′ axis; the intersection with Z′ axis, represents the sample bulk resistance, R_b. It is also clear that the circle diameter decreases with increasing salt concentration. The values of bulk conductivity σ_b of the polymer composites were obtained ($\sigma_b = d/R_bA$, where d is the film thickness and A is its effective area) for different ratios of C in the polymer electrolyte.

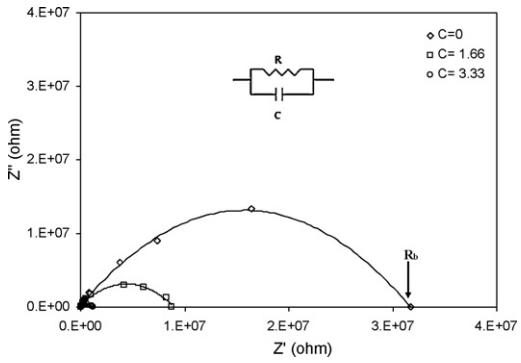

Fig. 4. Impedance plots (Cole–Cole plots) for PVA: C (NaI/$CuCl_2$) polymer electrolytes at room temperature.

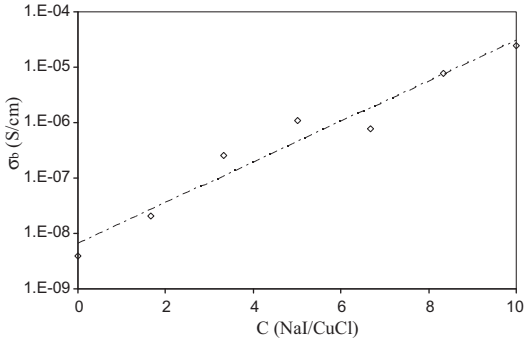

Fig. 5. The dependence of σ_b on the concentration C = NaI/$CuCl_2$.

The values of σ_b increase exponentially with increasing C ratio, Fig. 5,

$$\sigma_b = \sigma_{bo} \exp\left(\frac{C}{C_o}\right) \quad (2)$$

where σ_{bo} is the bulk conductivity at $C = 0$ (PVA bulk conductivity) and C_o is the effective NaI/$CuCl_2$ ratio (the onset of salt conductivity enhancement). The values of σ_{bo} and C_o are obtained by least square fitting of Eq. (2); they are equal to 7×10^{-9} S cm^{-1} and 1.19, respectively. The value of C_o is lower than the expected reactivity C ratio (= 1.75) which can be attributed to the complexation of NaI in the PVA matrix.

The conductivity of the present polymer electrolyte can be explained as, at low concentration of CuI, the conductivity is mainly due to the host polymer matrix. As the concentration of CuI phase increases beyond C_o, the conductivity is due to hole conduction in CuI crystallites besides oxidation/reduction iodine in polymer matrix. In other words as the C ratio increases, an excess of NaI dissolved in the polymer matrix contribute with the positive holes of CuI particles in conduction process.

The frequency dependence of the total conductivity $\sigma_{tot}(\omega)$ for the polymer electrolyte at 303 K is shown in Fig. 6, which follows a universal power law [13],

$$\sigma_{tot}(\omega) = \sigma_{dc} + A\omega^s \quad (3)$$

where σ_{dc} is the dc conductivity (the extrapolation of the plateau region to zero frequency), A is frequency independent pre-exponential factor, ω is the angular frequency and s is the frequency exponent. In addition the relation of $\sigma_{tot}(\omega)$ against frequency shifts upward with increasing C ratio and the kink shifts toward higher frequency range. The values of the exponent s have been obtained using the least square fitting, it can be observed that the exponent s decreases with increasing temperature and its value lies in the range $0.026 < s < 0.73$. Accordingly, these results lead to the

Please cite this article in press as: E. Sheha, et al., Structure, dielectric and optical properties of p-type (PVA/CuI) nanocomposite polymer electrolyte for photovoltaic cells, Optik - Int. J. Light Electron Opt. (2011), doi:10.1016/j.ijleo.2011.06.066

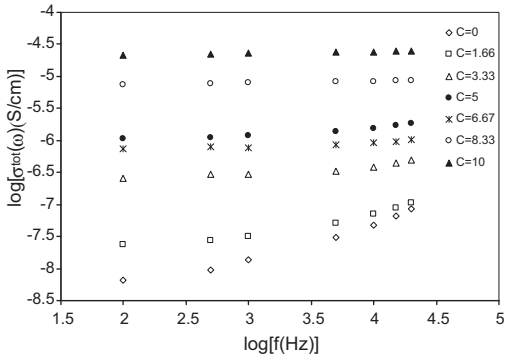

Fig. 6. Frequency dependent conductivity for PVA: C ($NaI/CuCl_2$) polymer electrolytes at room temperature.

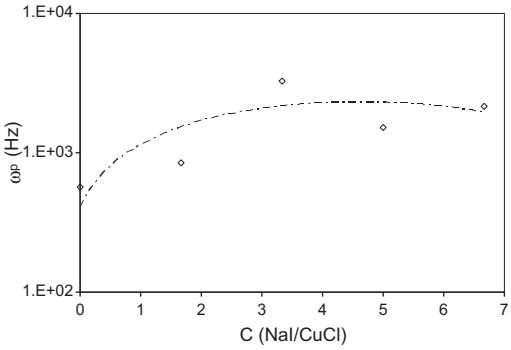

Fig. 7. Variation of the hopping rate ω_p with the concentration of C ratio.

prediction that the domination of ionic component in hopping conduction which is the most suitable mechanism to explain the ac conduction behavior in these polymer electrolyte [14].

In addition the transition between the nearly frequency independent region (dc conductivity) at low frequencies and that at intermediate frequencies (polarizing conductivity) may occur at a certain frequency ω_p (defined as the hopping rate). This rose from the competition of both dc conductivity and that due to the ionic polarization besides the electronic one. The values of ω_p are obtained by assuming that the ac conductivity is nearly equal to dc conductivity at $\omega = \omega_p$ [15],

$$\omega_p = \left(\frac{\sigma_{dc}}{A}\right)^{1/n} \tag{4}$$

The obtained values of ω_p shift to higher frequencies with increasing C ratio obeying the following empirical relation,

$$\omega_p = aC^2 + bC + d \tag{5}$$

where a, b, and d are fitting parameters. The plot of ω_p against C shown in Fig. 7, shows maximum at 3.85 which indicates that as the ratio C increases the hopping rate increases up to 3.85 due to the increase of salt phase CuI and the excess of NaI which lead to decreasing of the particle separation distance (hopping distance).

Fig. 8 illustrates the temperature dependence of bulk conductivity σ_b at different C ratio which can be described by the following Arrhenius equation

$$\sigma_b T = \sigma_{bo} \exp\left(\frac{E_b}{KT}\right) \tag{6}$$

where E_b is the bulk conductivity activation energy. The values of E_b are obtained by least square fitting of Eq. (6) and listed in Table 1. It is clearly observed that E_b decreases, where the value of bulk conductivity increases, with increasing C ratio. Druger

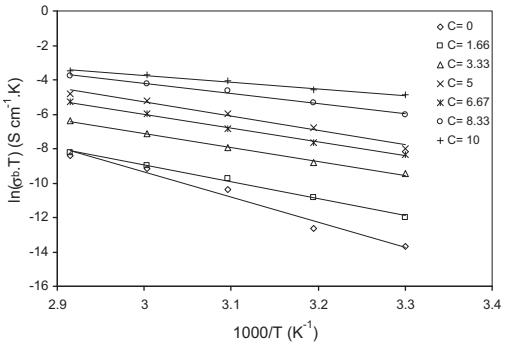

Fig. 8. Temperature dependent bulk conductivity σ_b for PVA: C ($NaI/CuCl_2$) polymer electrolytes.

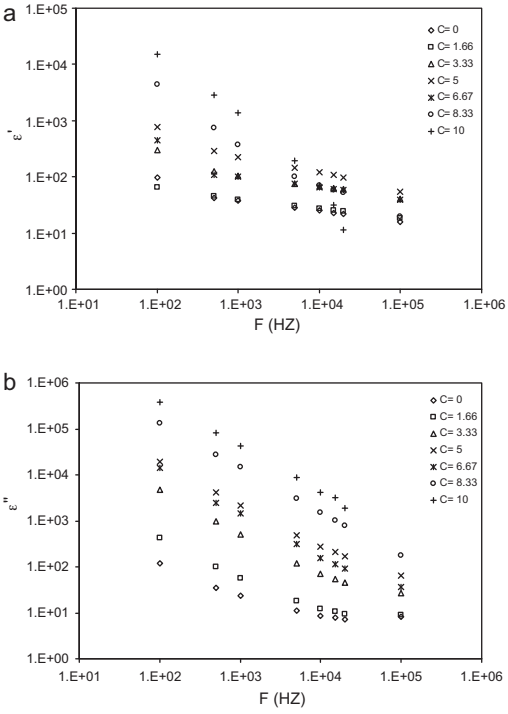

Fig. 9. Variation of (a) dielectric constant ε', (b) dielectric loss ε'' with frequency for PVA: C ($NaI/CuCl_2$) polymer electrolytes at 303 K.

et al. [16] have attributed the increase in conductivity with temperature in solid polymer electrolyte to segmental (i.e. polymer chain) motion, which results in an increase in the free volume of the system. This, in turns, results in the ions to hop from one site and provides a pathway for ions to move. In other words, the segmental movement of the polymer facilitates the translational ionic motion. From this, it is clear that the ionic motion is due to translational motion/hopping facilitated by the dynamic segmental motion of the polymer, the increase of charge carrier mobility. As the matrix amorphicity increases the polymer chain acquires faster internal modes in which bond rotations produce segmental motion to favor inter and intra-chain ion hopping, and thus the degree of conductivity becomes high. Frequency- and temperature-dependent conductivity is caused by the hopping of the charge carriers in the localized states and also due to the excitation of the charge Carriers to the states in the conduction band [17].

Fig. 9(a and b) shows the variation of the dielectric permitivity ε' and dielectric loss ε'' versus frequency respectively at room temperature, 303 K. Both ε' and ε'' decrease monotonically with increasing

Please cite this article in press as: E. Sheha, et al., Structure, dielectric and optical properties of p-type (PVA/CuI) nanocomposite polymer electrolyte for photovoltaic cells, Optik - Int. J. Light Electron Opt. (2011), doi:10.1016/j.ijleo.2011.06.066

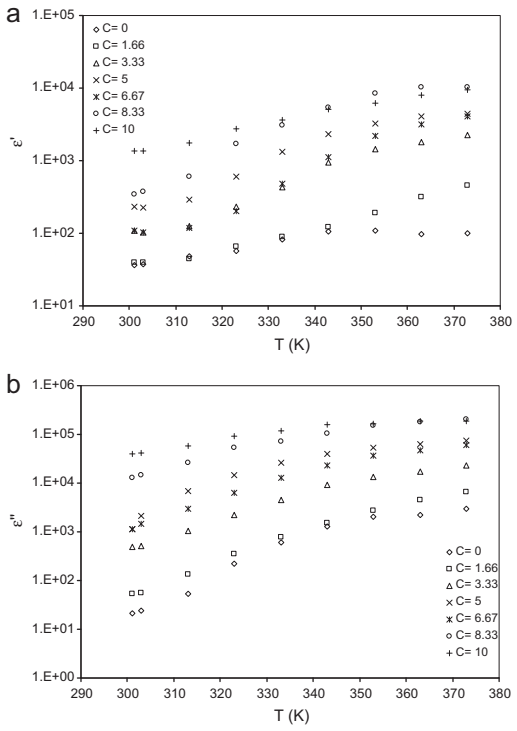

Fig. 10. Variation of (a) dielectric constant ε', (b) dielectric loss ε'' with temperature for PVA: C (NaI/$CuCl_2$) polymer electrolytes at 1 kHz.

frequency in the frequency range of $\omega\tau >> 1$. This behavior can be described by the Debye dispersion relations [18]:

$$\varepsilon' \cong \varepsilon_\infty + \frac{\varepsilon_s - \varepsilon_\infty}{1+\omega^2\tau^2}, \quad \varepsilon'' \equiv \frac{(\varepsilon_s - \varepsilon_\infty)\omega\tau}{1+\omega^2\tau^2} \tag{7}$$

where ε_∞ and ε_s are the static and infinite dielectric permittivities, τ is the relaxation time and ω is the angular frequency. The decrease of ε' and ε'' with frequency can be associated to the inability of dipoles to rotate rapidly leading to a lag between frequency of oscillating dipole and that of applied field. The variation indicates that at low frequencies the dielectric constant is high due to the interfacial polarization and the dielectric loss (ε'') becomes very large at lower frequencies due to free charge motion within the material [19].

Fig. 10(a and b) shows the variation of the dielectric constant ε' and dielectric loss ε'' versus temperature T, at constant frequency 1 kHz. It is clear that ε' and ε'' increases with increase temperature. This behavior is typical of polar dielectrics in which the orientation of dipoles is facilitated with the rising temperature and thereby the permittivity is increased [20].

3.4. Optical absorption studies

The optical absorption spectrum is an important tool to obtain optical energy band gap of crystalline and amorphous materials. The fundamental absorption, which corresponds to the electron excitation from the valance band to the conduction band, can be used to determine the nature and value of the optical band gap. Concerning the optical transitions resulting from photons of energy $h\upsilon \succ E_g$, the present optical data can be investigated according to the following relation ship for the near edge optical absorption [21],

$$(\alpha h\upsilon)^{1/n} = A(h\upsilon - E_g) \tag{8}$$

where α is the absorption coefficient, υ is the frequency, h is the Planck's constant, A is a constant, E_g is the optical energy band gap between the valence and the conduction bands and n is the power

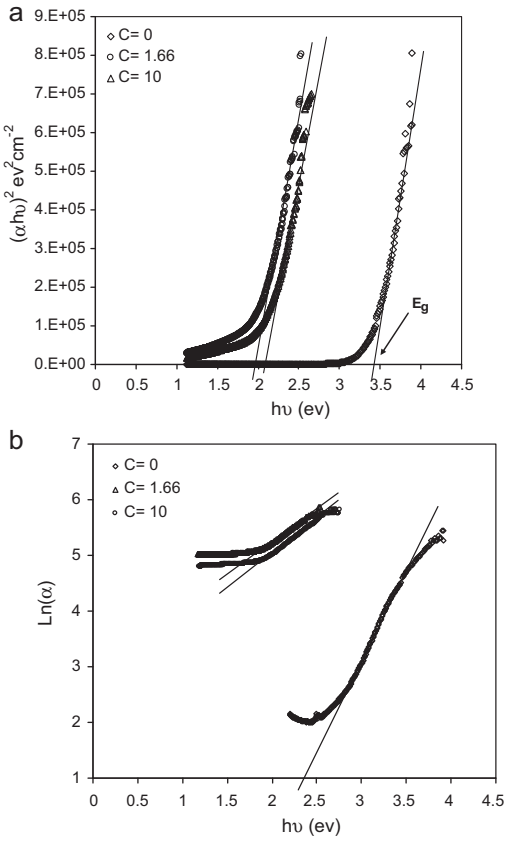

Fig. 11. The dependence of (a) $(\alpha h\upsilon)^2$, (b) $Ln(\alpha)$ on the photon energy $h\upsilon$.

that characterizes the transition process, where it is equal to 1/2 for direct allowed transition. The direct band gaps were obtained from the linear portion of $(\alpha h\upsilon)^2$ vs. $h\upsilon$ plot as shown in Fig. 11(a), the values of E_g obtained are given in Table 1. From the table we find that the increase of salt concentration has been small significant change on the optical gap width which mainly depends on the CuI particle size in the polymer matrix. As the size of semiconductor particles decreases to the nanoscale, the band gap of the semiconductor increases, causing a blue shift in the UV–vis absorption spectra due to quantum confinement [22].

On the other hand, for optical transitions caused by photons of energy $h\upsilon \prec E_g$, the absorption of photons will be related to the presence of localized tail states in the forbidden gap. The width of this tail, the Urbach tail, is an indicator of the defect levels in the forbidden band gap. The following relation was used to calculate the width of the Urbach tail [23]

$$\alpha = \alpha_o \ \exp\left(\frac{h\upsilon}{E_u}\right) \tag{9}$$

where α_o is constant and the Urbach tail E_u was determined from the slope of the straight lines of $Ln(\alpha)$ versus photon energy $h\upsilon$ of Fig. 11(b). The results of E_u are given in Table 1.

The magnitudes of E_b obtained from conductivity data are small in comparison with optical band gap energies. This is due to the fact that their nature is different. While the activation energy corresponds to the energy required for conduction from one site to another, the optical band gap corresponds to interband transition.

4. Conclusion

Synthesis of CuI by means of reducing $CuCl_2$ by NaI in an aqueous PVA solution succeeded and resulted in a p-type semiconductor nanocomposite (i.e. PVA/CuI). XRD results indicated the hexagonal

Please cite this article in press as: E. Sheha, et al., Structure, dielectric and optical properties of p-type (PVA/CuI) nanocomposite polymer electrolyte for photovoltaic cells, Optik - Int. J. Light Electron Opt. (2011), doi:10.1016/j.ijleo.2011.06.066

phase of CuI nanoparticles were formed within the PVA matrix. The optical absorption measurements indicate that the absorption mechanism is due to allowed direct transitions for all samples. The optical band gap and Urbach energy values change with the change in the particle size of CuI and its concentration inside the polymer matrices and due to quantum confinement. Activation energy values obtained from the conductivity data were in the range 0.33–1.24 eV. This type of electrolyte could thus be a suitable candidate for photovoltaic cells, although a further enhancement in ionic conductivity, especially at the lowest temperature, is desired.

References

[1] D.Y. Godovsky, Device applications of polymer nanocomposites, Adv. Polym. Sci. 153 (2000) 163–205.
[2] K.A. Abdelkader, Z. Anwar, Spectroscopic studies of poly vinyl alcohol, J. Appl. Polym. Sci. 2 (2006) 1146–1151.
[3] K. Tennakone, G.R.R.A. Kumara, I.R.M. Kottegoda, V.P.S. Perera, G.M.L.P. Aponsu, K.G.U. Wijayantha, Deposition of thin conducting films of CuI on glass, Sol. Energy Mater. Sol. Cells 55 (1998) 283–289.
[4] G.R.R.A. Kumara, A. Konno, G.K.R. Senadeera, P.V.V. Jayaweere, D.B.R.A. De Silva, T. Tennakone, Dye-sensitized solar cell with the hole collector P-CuSCN deposited from a solution in *n*-propyl sulphide, Sol. Energy Mater. Sol. Cells 69 (2001) 195–199.
[5] K. Tonooka, K. Shimokawa, O. Nishimura, Properties of copper–aluminum oxide films prepared by solution methods, Thin Solid Films 411 (2002) 129–133.
[6] S.L. Dhere, S.S. Latthe, C. Kappenstein, S.K. Mukherjee, A.V. Rao, Comparative studies on P-Type CuI grown on glass and copper substrate by SILAR method, Appl. Surf. Sci. 256 (2010) 3967–3971.
[7] C.B. Murray, C.R. Kagan, M.G. Bawendi, Self-organization of CdSe nanocrystallites into three-dimensional quantum dot superlattices, Science 270 (1995) 1335–1338.
[8] P.V. Kamat, Interfacial charge transfer processes in colloidal semiconductor systems, Prog. React. Kinet. 19 (1994) 277–316.
[9] B.Z. Tang, Y. Geng, J.W.Y. Lam, B. Li, X. Jing, X. Wang, F. Wang, A.B. Pakhomov, X.X. Zhang, Processible nanostructured materials with electrical conductivity and magnetic susceptibility: preparation and properties of maghemite/polyaniline nanocomposite films, Chem. Mater. 11 (1999) 1581–1589.
[10] Z. Changneng, K. Mingguang, Z. Xiaoguang, W. Kongjia, W. Mingtai, L. Fang, G. Li, X. Weiwei, A polymeric/inorganic nanocomposite for solid-state dye-sensitized solar cells, Plasma Sci. Technol. 7 (2005) 2962–2964.
[11] R.M. Hodge, G.H. Edward, G.P. Simon, Water absorption and states of water in semicrystalline poly (vinyl alcohol) films, Polymer 37 (1996) 1371–1376.
[12] B. Pejova, I. Grozdanov, Three-dimensional confinement effects in semiconducting zinc selenide quantum dots deposited in thin-film form, Mater. Chem. Phys. 90 (2005) 35–46.
[13] T. Winie, A.K. Arof, Dielectric behaviour and AC conductivity of $LiCF_3SO_3$ doped H-chitosan polymer films, Ionics 10 (2004) 193–199.
[14] F.H. Abd El-kader, W.H. Osman, K.H. Mahmoud, M.A.F. Basha, Dielectric investigations and ac conductivity of polyvinyl alcohol films doped with europium and terbium chloride, Physica B 403 (2008) 3473–3484.
[15] M.K. E1-Mansy, Electrical conduction and dielectric relaxation in vanadium phosphate glasses, Mater. Chem. Phys. 56 (1998) 236–242.
[16] S.D. Druger, A. Nitzam, M.A. Ratner, Dynamic bond percolation theory: a microscopic model for diffusion in dynamically disordered systems. I. Definition and one dimensional case, J. Chem. Phys. 79 (1983) 3133–3143.
[17] V. Raja, A.K. Sharma, V.V.R. Narasimha Rao, Impedance spectroscopic and dielectric analysis of PMMA-CO-P4VPNO polymer films, Mater. Lett. 58 (2004) 3242–3247.
[18] E. Nora, Hill, et al., Dielectric Properties and Molecular Behavior, Van Nostrand, London, 1969.
[19] A. Kyritsis, P. Pissis, J. Grammatikakis, Dielectric relaxation spectroscopy in poly(hydroxyethyl acrylates)/water hydrogels, J. Polym. Sci. Part B: Polym. Phys. 33 (1995) 1737–1750.
[20] B. Tareev, Physics of Dielectric Materials, MIR Publications, Moscow, 1979.
[21] Y. Aydogdu, F. Yakuphanoglu, A. Aydogdu, E. Tas, A. Cukuraval, Electrical and optical properties of newly synthesized glyoxime complexes, Solid State Sci. 4 (2002) 879–883.
[22] H. Wang, P. Fang, Z. Chen, S. Wang, Synthesis and characterization of CdS/PVA nanocomposite films, Appl. Surf. Sci. 253 (2007) 8495–8499.
[23] A. El-Khodary, Evolution of the optical, magnetic and morphological properties of PVA films filled with $CuSO_4$, Physica B 405 (2010) 3401–3408.

Please cite this article in press as: E. Sheha, et al., Structure, dielectric and optical properties of p-type (PVA/CuI) nanocomposite polymer electrolyte for photovoltaic cells, Optik - Int. J. Light Electron Opt. (2011), doi:10.1016/j.ijleo.2011.06.066